Published in final edited form as:
J Thorac Oncol. 2014 November ; 9(11): 1698–1703. doi:10.1097/JTO.0000000000000319.

Noninvasive Risk Stratification of Lung Adenocarcinoma using Quantitative Computed Tomography

Sushravya Raghunath, PhD[1,3], **Fabien Maldonado, MD**[2], **Srinivasan Rajagopalan, PhD**[1], **Ronald A. Karwoski**[1], **Zackary S. DePew, MD**[2], **Brian J. Bartholmai, MD**[3], **Tobias Peikert, MD**[2], and **Richard A. Robb, PhD**[1]

[1]Department of Physiology and Biomedical Engineering, Mayo Clinic, Rochester MN

[2]Division of Pulmonary and Critical Care Medicine, Mayo Clinic, Rochester MN

[3]Department of Radiology, Mayo Clinic, Rochester MN

Abstract

Introduction—Lung cancer remains the leading cause of cancer-related deaths in the US and worldwide. Adenocarcinoma is the most common type of lung cancer and encompasses lesions with widely variable clinical outcomes. In the absence of noninvasive risk stratification, individualized patient management remains challenging. Consequently a subgroup of pulmonary nodules of the lung adenocarcinoma spectrum is likely treated more aggressively than necessary.

Methods—Consecutive patients with surgically resected pulmonary nodules of the lung adenocarcinoma spectrum (lesion size ≤ 3 cm, 2006–2009) and available pre-surgical high-resolution computed tomography (HRCT) imaging were identified at Mayo Clinic Rochester. All cases were classified using an unbiased Computer-Aided Nodule Assessment and Risk Yield (CANARY) approach based on the quantification of pre-surgical HRCT characteristics. CANARY-based classification was independently correlated to postsurgical progression-free survival.

Results—CANARY analysis of 264 consecutive patients identified three distinct subgroups. Independent comparisons of 5-year disease-free survival (DFS) between these subgroups demonstrated statistically significant differences in 5-year DFS, 100%, 72.7% and 51.4%, respectively ($p = 0.0005$).

Conclusions—Non-invasive CANARY based risk stratification identifies subgroups of patients with pulmonary nodules of the adenocarcinoma spectrum characterized by distinct clinical outcomes. This technique may ultimately improve the current expert opinion-based approach to the management of these lesions by facilitating individualized patient management.

Introduction

With an estimated 224,210 new cases and 159,260 deaths in 2014[1], lung cancer remains the leading cause of cancer-related mortality in the United States (US). While early diagnosis

Corresponding author: Sushravya Raghunath, PhD, RO_BIR, 200 1st Street SW, Rochester, MN, 55904, Ph: 507-284-3068, Raghunath.sushravya@mayo.edu.

offers a chance of cure, the majority of patients are diagnosed with advanced stage disease associated with extremely poor outcomes. Based on the 20% relative reduction in lung cancer-specific mortality observed in the National Lung Screening Trial (NLST)[2], the US Preventive Services Task Force has issued recommendations in favor of High-Resolution Computed Tomography (HRCT)-based screening[3]. Consequently, lung cancer screening programs are being implemented across the US[4–7]. However, in addition to the early detection of aggressive lung cancers, screening also leads to the detection of a substantial proportion of "overdiagnosed" lung cancers, i.e. cancers unlikely to impact the overall survival of patients regardless of management [3, 8, 9]. This could represent a substantial problem as an estimated 10.6 million individuals would be eligible for HRCT screening in the US alone based on NLST criteria.

Lung adenocarcinoma is the most common type of lung cancer. It typically presents as persistent solitary or multifocal, solid or subsolid nodules on HRCT. Histologically, adenocarcinomas consist of various combinations of lepidic growth (non-invasive tumor cell growth along intact alveolar septa) and tissue invasion, corresponding generally to areas of ground-glass attenuation and solid density, respectively on HRCT [10–12].

While most lung adenocarcinomas are aggressive, some have a more indolent course, clinically asymptomatic incidentally or screen-detected represent the majority of potentially overdiagnosed lesions. Current treatment strategies are predominantly based on the size and location of the lesions, without assessment of lesion-specific aggressiveness, which may result in overtreatment (treatment of an otherwise asymptomatic indolent lesion) leading to unnecessary morbidity, mortality and healthcare expenses.[2, 8, 9, 13, 14]. Specifically, adenocarcinomas in situ (AIS) and minimally invasive adenocarcinomas (MIA) are characterized by excellent (almost 100%) postsurgical 5-year survival, whereas invasive adenocarcinomas (IA) have worse prognosis.[15, 16] These differences in clinical outcome are reflected in the recently updated classification of lung adenocarcinomas, which is based on the semi-quantitative histologic assessment of these lesions[16]. In addition to clinical-pathological disease staging (**T**umor-**N**ode-**M**etastasis (TNM) staging), comprehensive histological assessment represents the most powerful outcome predictor for these patients[16, 17]. Assuming that we can infer the biological behavior of these lesions from these post-treatment outcomes, non-invasive assessment through HRCT classification could ultimately assist in the selection of alternative treatment strategies. However, currently risk assessment and tumor behavior prediction is limited to surgically resected lesions. Comprehensive histopathological assessment is not possible with small bronchoscopic or CT-guided biopsies and no other non-invasive or minimally invasive biomarkers help to guide preoperative treatment strategies. Robust and reproducible non-invasive pretreatment risk-stratification strategies are therefore urgently needed.

Computer-Aided Nodule Assessment and Risk Yield (CANARY) is a novel software application developed at Mayo Clinic, which allows automated HRCT-based quantitative characterization of pulmonary nodules[18]. We previously reported the excellent correlation between HRCT-based CANARY signatures and semi-quantitative histology analysis. Herein we report a new CANARY-based risk stratification approach for pulmonary nodules of the adenocarcinoma spectrum. This non-invasive approach is independent of histologic

assessment and addresses inherent limitations of histology such as inter-observer variability and intra-tumor heterogeneity[19].

Materials and Methods

Data

We retrospectively identified consecutive patients with surgically resected solitary lung adenocarcinomas and an available preoperative HRCT (within 3 months of surgery) between January 2006 and December 2007. In addition, we included all consecutive cases with clinically stage I solitary pulmonary nodules (≤ 3cm) resected between January 2008 and December 2009. Clinical data including disease free survival (DFS) was collected from the Mayo Clinic electronic medical records. The study was approved by the Mayo Clinic IRB.

Nodule characterization and CANARY development

The development of CANARY has been described in detail[18]. Briefly, a thoracic chest radiologist (BJB) arbitrarily selected 774 regions of interest (ROIs, 9×9 voxels) spanning the spectrum of radiologic appearance of adenocarcinomas (form pure groundglass to pure solid) in 37 randomly selected pulmonary nodules. The similarity of the radiologic features between ROIs was compared using a pairwise similarity metric and nine characteristic ROI clusters (i.e. groups of radiologically similar ROIs) and corresponding “ROI exemplars” were identified using Affinity Propagation (AP)[20], an unsupervised clustering algorithm. Unlike other clustering algorithms, AP does not require the number of clusters to be specified prior to analysis i.e., it identifies natural clusters with their most representative data point within the dataset. The nine ROI exemplars were color-coded as violet (V), indigo (I), blue (B), green (G), yellow (Y), orange (O), red (R), cyan (C) and pink (P) and represent the basic building blocks of nodules of the adenocarcinoma spectrum. Nodules are analyzed by sequential analysis of each voxel within the nodule of interest. Each voxel (with its surrounding 80 voxels in a 9×9 voxel ROI) is compared to the nine identified ROI exemplars, and the color code of the most similar ROI exemplar is assigned to the analyzed voxel. The adjacent voxel is then analyzed in a similar fashion until all voxels contained in the nodule of interest have been color-coded, yielding a specific *parametric signature* for the nodule. This methodology and the parametric signatures have previously been validated by consensus histology of resected nodules in the adenocarcinoma spectrum[18].

Nodule categorization and quantitative unsupervised stratification

Given the correlation of histologic analysis with survival characteristics in pulmonary adenocarcinoma, we hypothesized that CANARY-based parametric signatures of these nodules would correlate with prognosis, independent of histology. Specifically, we postulated that the distribution of the 9 ROI exemplars within individual nodules would correlate with the risk of disease progression, independent of histology or clinical input, similar in that way to the comprehensive histological assessment[17] described in the updated classification of adenocarcinomas[16]. To that end, we applied the same clustering algorithm (AP) to identify natural clusters within the cohort of CANARY analyzed nodules to determine the type and number of groups of radiologically similar nodules based on the

CANARY parametric signatures that constitute those nodules. DFS was compared between the resulting groups.

Nodule Exemplars—AP was used to identify natural clusters (clusters with similar distribution of parametric signatures) among lung adenocarcinomas. The most representative nodule or "nodule exemplar" was identified within each cluster that served as the reference for the cluster.

Nodule categorization—All included clinical stage I solitary pulmonary nodules were categorized into one of the identified clusters by comparing the mathematical similarity *(details in* supplementary methods) of each nodule with the naturally identified nodule exemplars.

Cluster Analysis—The quantitative efficacy of the stratification was assessed for statistical significance using Analysis of Similarity (ANOSIM)[21].

Survival Analysis

Follow-up data was collected retrospectively and post-operative follow-up was not standardized. As reflected by the divergence in the guideline recommendations by different professional organizations follow-up visits and imaging modalities varied based on provider preferences[22–27]. The majority of patients had follow-up at Mayo Clinic. In general patients were seen more commonly (every 3–6 months) during the first 2 years and every 6 months between 3–5 years. The median follow-up was 3.07 years (last update: Dec 2013). Chest CT was the most commonly used imaging modality for follow-up. As expected, the majority of recurrences were distant metastasis rather than pulmonary recurrences/metastasis. Deaths due to clearly documented other causes, in the absence of any evidence for recurrent disease, were censored at the time of death. There were a total of 27 such events in the study cohort.

Kaplan-Meier analysis (GraphPad Prism version 5.00 for Microsoft Windows, GraphPad Software, San Diego, California, USA) was performed to compare the DFS of the identified groups. The curves were compared using log-rank statistical test. Cox proportional hazard fit (JMP 10.0.0, SAS) was performed to form the multivariate model accounting for age, gender, smoking (never vs current/former), histologic staging and stratified clusters. All patients had R0 surgical resections (curative resection) and clinical progression was defined as pathologically confirmed disease recurrence, as assessed by consensus of 3 of the author investigators (F.M., T.P. and Z.S.D.). The patients were censored at the time of their last follow-up in the absence of disease recurrence. P-values < 0.05 were considered significant.

Results

Patients

Three-hundred-six patients with surgically resected lung adenocarcinomas, January 2006 to December 2009 at Mayo Clinic, Rochester, MN were included in our study. This included 264 cases of clinically Stage I solitary pulmonary nodules. Demographic information and pathological tumor stages of these cases are summarized in Table 1.

Quantitative Nodule Characterization and Visualization

CANARY-based characterization of representative resected adenocarcinomas is illustrated in Figure 1. The glyphs represent a quantitative summary of the respective distribution of the ROI exemplars within each nodule. The radius of each glyph is set proportional to the volume of the nodule

Quantitative Nodule Categorization

The AP clustering using 170 cases of lung adenocarcinoma including 128 clinical Stage I pulmonary nodules (2006–2007) yielded three natural clusters from which the three nodule exemplars were identified, and were secondarily found to represent predominantly B-G-C (i), mixed (ii) and predominantly V-I-R-O nodules (iii). Figure 2 shows the CT sections, color-coded patterns and glyphs for the three nodule exemplars. ANOSIM yielded R = 0.6930 with p-value = 0.001. Internal validation was successfully performed using leave-one-out (LOO) and k-fold (k = 10) cross validation (CV) techniques (*details in* supplementary methods).

Correlation with DFS

All 264 clinical Stage I pulmonary nodules of the lung adenocarcinoma spectrum were categorized into the identified three clusters. This categorization was statistically significant (ANOSIM R = 0.59; p-value = 0.001). DFS was extracted in a blinded fashion and analyzed for these three clusters using Kaplan-Meier statistics. This analysis yielded 100%, 72.7% and 51.4%, 5-year DFS for the three groups respectively (log-rank test p = 0.0005). Figure 3 shows the DFS curves. Based on this analysis the three groups were labeled as good (G), intermediate (I) and poor (P) risk. The log-rank test and univariate Mantel-Haenszel Hazard ratios (HR) revealed statistically significant differences between groups G and I with p-value = 0.0055 (HR: 3.47 [1.44 to 8.22]); groups G and P with p-value = 0.0002 (HR: 5.338 [2.23 to 12.78]) and groups I and P with p-value = 0.02 (HR: 2.02 [1.10 to 3.73]). Table 2 summarizes the multivariate cox proportional model using likelihood ratio tests for the stratified groups adjusted for age, gender, smoking history and histologic staging as covariates.

Discussion

In the present study, we report the use of a novel HRCT-based imaging biomarker for the noninvasive risk stratification of lung adenocarcinoma. We have identified three clusters of adenocarcinomas that naturally segregate using AP based on HRCT characteristics. Each of these clusters correlates strongly with the post-surgical DFS. Unlike other stratification approaches,[28] we did not use an outcome-matched trained model but identified these clusters independently of clinical data. Furthermore, in contrast to methods that differentiate lung nodules based on their HRCT appearance using various combinations of multiple quantitative features[29, 30] we used a single, robust similarity metric for objective risk stratification. The three identified groups corresponded to good (G), intermediate (I) and poor (P) postoperative DFS. This strategy potentially facilitates the non-invasive classification of nodules prospectively in new patients. Inferring biological behavior based on these known post-treatment outcomes, HRCT-based CANARY classification could

ultimately guide the individualized management of these lesions. For example, nodules non-invasively categorized as 'Good,' representing indolent lesions, could benefit from less aggressive surgical approaches, non-invasive or minimally invasive therapy or watchful waiting while nodules that have characteristics corresponding to the more aggressive lesions (P group) would be managed with current standard of care, such as lobectomy, and perhaps additional adjuvant therapy. The introduction of lung cancer screening is expected to result in a substantial increase in screening-detected lung cancers. Early detection is projected to decrease lung cancer specific mortality; however an estimated 20% of patients with screening-detected lung cancer, almost exclusively adenocarcinomas, will potentially be overdiagnosed[9]. This phenomenon could result in increased morbidity, mortality and health care costs. In comparison to strategies mitigating the impact of false-positive pulmonary nodules, preoperative non-invasive risk stratification of pulmonary nodules of the lung adenocarcinoma spectrum has been less well studied. Effective biomarkers to discriminate aggressive from indolent lesions are urgently needed[3, 31]. Current therapeutic management decisions for these nodules currently rely on low-level evidence and expert opinion[12]. For example, the selection of patients for limited surgical resection in ongoing clinical trials is largely restricted to lesion size, highlighting the need for accurate and consistent interpretation tools[32]. Ideally, treatment strategies including standard lobectomy, limited local resection (wedge or segmentectomy), stereotactic body radiation therapy and watchful waiting[33, 34] should be individualized based on the aggressiveness of the lesion.

Thus far quantitative imaging efforts for lung nodules have generally focused on nodule detection strategies[35–38]. Several CT-based techniques have been explored to characterize pulmonary nodules[39–42]. The majority of these studies focus exclusively on solid nodules. They utilize the shape characteristics like spiculation, nodule eccentricity, volume and largest diameter. Correlation of these strategies with histology and survival has been inconsistent[42, 43].

In real-world clinical practice, the variable HRCT acquisition techniques, methods of image reconstruction and filtering from different CT scanner equipment can have enormous effects on the visual appearance of images and the quantitative characteristics of the pixels. To overcome some of the potential variability and assure that quantitative results are valid, an assessment of algorithm performance across multiple different types of input is required. Our preliminary assessment suggests CANARY represents a robust risk stratification tool that can be utilized on a variety of HRCT techniques for retrospective or prospective evaluation of lung nodules in a real-world setting. Specifically, our results are consistent across a wide variety of clinically utilized CT protocols performed on various types of equipment. The stability of CANARY characterization and stratification of scans reconstructed with sharp and smooth filtering algorithms are shown in **Figure E1**. Additional work to assess the specific limitations of CANARY parametric signature quantification with regard to the effects of slice thickness, reconstruction methodology and other factors such as noise or dose-related changes in image characteristics may be warranted.

Our current report represents, to our knowledge, the first attempt using population imaging data and quantified radiologic characteristics to identify distinct clusters of lesions characterized by similar biologic behavior.

We acknowledge that prognostication based on a single time point is uncertain[44] and the estimate of prognosis for an individual patient may change over time. As such, the application of CANARY over time will promote our understanding of the natural history of pulmonary nodules of the lung adenocarcinoma spectrum. Determination of the rate of transition from indolent to aggressive characteristics or confident quantification of stability may enable timely appropriate management of lesions through non-invasive HRCT assessment. With additional validation, we expect that this method will facilitate individualized follow-up and management of pulmonary nodules of the lung adenocarcinoma in a standardized, objective fashion.

Supplementary Material

Refer to Web version on PubMed Central for supplementary material.

Acknowledgments

Sources of support: K23 award (K23CA159391-01A1) – Dr. Tobias Peikert.

Center of Individualized Medicine (CIM), Mayo Clinic.

Mayo Graduate School, Mayo Clinic – Dr. Sushravya Raghunath.

References

1. Society AC. Cancer Facts and Figures 2014. Atlanta: American Cancer Society; 2014.
2. Aberle DR, Adams AM, et al. National Lung Screening Trial Research T. Reduced lung-cancer mortality with low-dose computed tomographic screening. The New England journal of medicine. 2011; 365:395–409. [PubMed: 21714641]
3. Moyer VA. Screening for lung cancer: US Preventive Services Task Force recommendation statement. Annals of internal medicine. 2014
4. Bach PB, Mirkin JN, Oliver TK, et al. Benefits and harms of CT screening for lung cancer: a systematic review. JAMA: the journal of the American Medical Association. 2012; 307:2418–2429.
5. Jaklitsch MT, Jacobson FL, Austin JH, et al. The American Association for Thoracic Surgery guidelines for lung cancer screening using low-dose computed tomography scans for lung cancer survivors and other high-risk groups. The Journal of thoracic and cardiovascular surgery. 2012; 144:33–38. [PubMed: 22710039]
6. Wender R, Fontham ET, Barrera E Jr, et al. American Cancer Society lung cancer screening guidelines. CA: a cancer journal for clinicians. 2013; 63:107–117. [PubMed: 23315954]
7. Wood DE, Eapen GA, Ettinger DS, et al. Lung cancer screening. Journal of the National Comprehensive Cancer Network: JNCCN. 2012; 10:240–265. [PubMed: 22308518]
8. Veronesi G, Maisonneuve P, Bellomi M, et al. Estimating overdiagnosis in low-dose computed tomography screening for lung cancer: a cohort study. Annals of internal medicine. 2012; 157:776–784. [PubMed: 23208167]
9. Patz EF Jr, Pinsky P, Gatsonis C, et al. Overdiagnosis in Low-Dose Computed Tomography Screening for Lung Cancer. JAMA internal medicine. 2013
10. Detterbeck FC, Homer RJ. Approach to the ground-glass nodule. Clinics in chest medicine. 2011; 32:799–810. [PubMed: 22054887]

11. Godoy MC, Naidich DP. Subsolid pulmonary nodules and the spectrum of peripheral adenocarcinomas of the lung: recommended interim guidelines for assessment and management. Radiology. 2009; 253:606–622. [PubMed: 19952025]
12. Naidich DP, Bankier AA, MacMahon H, et al. Recommendations for the Management of Subsolid Pulmonary Nodules Detected at CT: A Statement from the Fleischner Society. Radiology. 2013; 266:304–317. [PubMed: 23070270]
13. Detterbeck FC, Gibson CJ. Turning gray: the natural history of lung cancer over time. Journal of thoracic oncology: official publication of the International Association for the Study of Lung Cancer. 2008; 3:781–792.
14. Takiguchi Y, Sekine I, Iwasawa S. Overdiagnosis in lung cancer screening with low-dose computed tomography. Journal of thoracic oncology: official publication of the International Association for the Study of Lung Cancer. 2013; 8:e101–102.
15. Nakata M, Saeki H, Takata I, et al. Focal ground-glass opacity detected by low-dose helical CT. Chest. 2002; 121:1464–1467. [PubMed: 12006429]
16. Travis WD, Brambilla E, Noguchi M, et al. International association for the study of lung cancer/american thoracic society/european respiratory society international multidisciplinary classification of lung adenocarcinoma. Journal of thoracic oncology: official publication of the International Association for the Study of Lung Cancer. 2011; 6:244–285.
17. Warth A, Muley T, Meister M, et al. The novel histologic International Association for the Study of Lung Cancer/American Thoracic Society/European Respiratory Society classification system of lung adenocarcinoma is a stage-independent predictor of survival. Journal of clinical oncology: official journal of the American Society of Clinical Oncology. 2012; 30:1438–1446. [PubMed: 22393100]
18. Maldonado F, Boland JM, Raghunath S, et al. Noninvasive characterization of the histopathologic features of pulmonary nodules of the lung adenocarcinoma spectrum using computer-aided nodule assessment and risk yield (CANARY)--a pilot study. Journal of thoracic oncology: official publication of the International Association for the Study of Lung Cancer. 2013; 8:452–460.
19. Marusyk A, Almendro V, Polyak K. Intra-tumour heterogeneity: a looking glass for cancer? Nat Rev Cancer. 2012; 12:323–334. [PubMed: 22513401]
20. Frey BJ, Dueck D. Clustering by passing messages between data points. science. 2007; 315:972–976. [PubMed: 17218491]
21. CLARKE KR. Non-parametric multivariate analyses of changes in community structure. Australian journal of ecology. 1993; 18:117–143.
22. Centers AoCC. Oncology patient management guidelines. Rockville, MD: 2000. version 3.0
23. Rubins J, Unger M, Colice GL, et al. Follow-up and surveillance of the lung cancer patient following curative intent therapy: ACCP evidence-based clinical practice guideline (2nd edition). Chest. 2007; 132:355S–367S. [PubMed: 17873180]
24. Sause WT, Byhardt RW, Curran WJ Jr, et al. Follow-up of non-small cell lung cancer. American College of Radiology. ACR Appropriateness Criteria. Radiology. 2000; 215 (Suppl):1363–1372. [PubMed: 11037552]
25. Pfister DG, Johnson DH, Azzoli CG, et al. American Society of Clinical Oncology treatment of unresectable non-small-cell lung cancer guideline: update 2003. Journal of clinical oncology: official journal of the American Society of Clinical Oncology. 2004; 22:330–353. [PubMed: 14691125]
26. Felip E, Stahel RA, Pavlidis N, et al. ESMO Minimum Clinical Recommendations for diagnosis, treatment and follow-up of non-small-cell lung cancer (NSCLC). Annals of oncology: official journal of the European Society for Medical Oncology/ESMO. 2005; 16 (Suppl 1):i28–29. [PubMed: 15888743]
27. Ettinger D, Bepler G, Bueno R, et al. Non-small cell lung cancer clinical practice guidelines in oncology. Journal of the National Comprehensive Cancer Network: JNCCN. 2006; 4:548. [PubMed: 16813724]
28. Cima I, Schiess R, Wild P, et al. Cancer genetics-guided discovery of serum biomarker signatures for diagnosis and prognosis of prostate cancer. Proceedings of the National Academy of Sciences of the United States of America. 2011; 108:3342–3347. [PubMed: 21300890]

29. Ravanelli M, Farina D, Morassi M, et al. Texture analysis of advanced non-small cell lung cancer (NSCLC) on contrast-enhanced computed tomography: prediction of the response to the first-line chemotherapy. European radiology. 2013
30. Gevaert O, Xu J, Hoang CD, et al. Non-small cell lung cancer: identifying prognostic imaging biomarkers by leveraging public gene expression microarray data--methods and preliminary results. Radiology. 2012; 264:387–396. [PubMed: 22723499]
31. Van Schil PE, Asamura H, Rusch VW, et al. Surgical implications of the new IASLC/ATS/ERS adenocarcinoma classification. The European respiratory journal. 2012; 39:478–486. [PubMed: 21828029]
32. Adjei AA. Lung cancer-celebrating progress and acknowledging challenges. Journal of thoracic oncology: official publication of the International Association for the Study of Lung Cancer. 2013; 8:1350–1351.
33. Gulati CM, Schreiner AM, Libby DM, et al. Outcomes of unresected ground-glass nodules with cytology suspicious for adenocarcinoma. Journal of thoracic oncology: official publication of the International Association for the Study of Lung Cancer. 2014; 9:685–691.
34. Chang B, Hwang JH, Choi YH, et al. Natural history of pure ground-glass opacity lung nodules detected by low-dose CT scan. Chest. 2013; 143:172–178. [PubMed: 22797081]
35. Roos JE, Paik D, Olsen D, et al. Computer-aided detection (CAD) of lung nodules in CT scans: radiologist performance and reading time with incremental CAD assistance. European radiology. 2010; 20:549–557. [PubMed: 19760237]
36. Messay T, Hardie RC, Rogers SK. A new computationally efficient CAD system for pulmonary nodule detection in CT imagery. Medical Image Analysis. 2010; 14:390–406. [PubMed: 20346728]
37. Awai K, Murao K, Ozawa A, et al. Pulmonary Nodules: Estimation of Malignancy at Thin-Section Helical CT—Effect of Computer-aided Diagnosis on Performance of Radiologists1. Radiology. 2006; 239:276–284. [PubMed: 16467210]
38. Bayarri MS, Suárez-Cuenca JJ, Tahoces PG, et al. Automatic detection of pulmonary nodules: Evaluation of performance using two different MDCT scanners. Journal of Biomedical Graphics & Computing. 2012:2.
39. McNitt-Gray MF, Hart EM, Wyckoff N, et al. A pattern classification approach to characterizing solitary pulmonary nodules imaged on high resolution CT: preliminary results. Medical physics. 1999; 26:880–888. [PubMed: 10436888]
40. Ye X, Lin X, Dehmeshki J, et al. Shape-based computer-aided detection of lung nodules in thoracic CT images. Biomedical Engineering, IEEE Transactions on. 2009; 56:1810–1820.
41. Way T, Chan H-P, Hadjiiski L, et al. Computer-Aided Diagnosis of Lung Nodules on CT Scans:: ROC Study of Its Effect on Radiologists' Performance. Academic radiology. 2010; 17:323–332. [PubMed: 20152726]
42. Kawata Y, Niki N, Ohmatsu H, et al. Quantitative classification based on CT histogram analysis of non-small cell lung cancer: Correlation with histopathological characteristics and recurrence-free survival. Medical physics. 2012; 39:988–1000. [PubMed: 22320808]
43. Tacelli N, Remy-Jardin M, Copin M-C, et al. Assessment of Non–Small Cell Lung Cancer Perfusion: Pathologic-CT Correlation in 15 Patients 1. Radiology. 2010; 257:863–871. [PubMed: 20843993]
44. Detterbeck F. Stage Classification and Prediction of Prognosis: Difference between Accountants and Speculators. Journal of thoracic oncology: official publication of the International Association for the Study of Lung Cancer. 2013; 8:820–822.

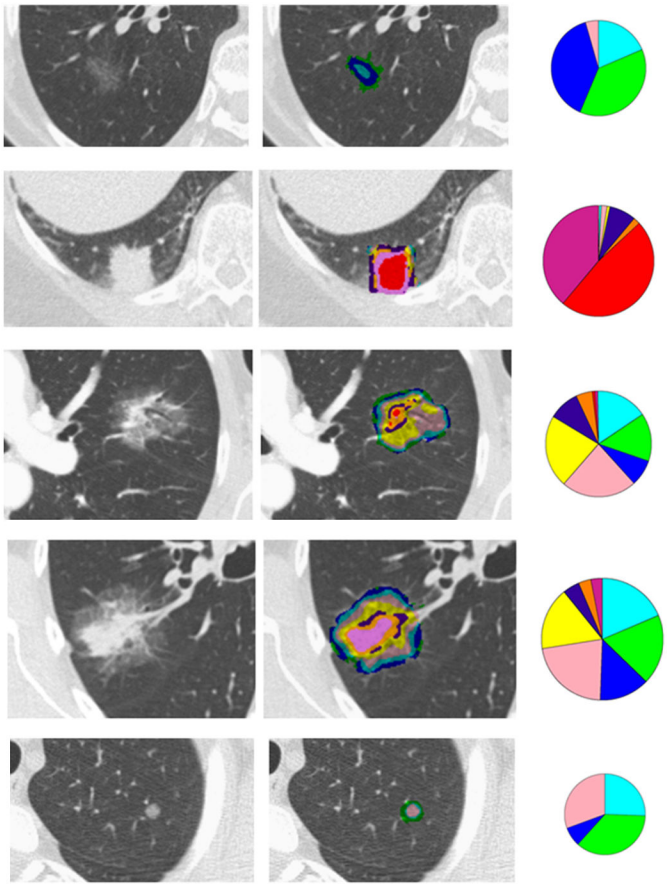

Figure 1.
The original CT axial sections, color-coded voxel classification overlay and glyph representations are shown for representative nodules.

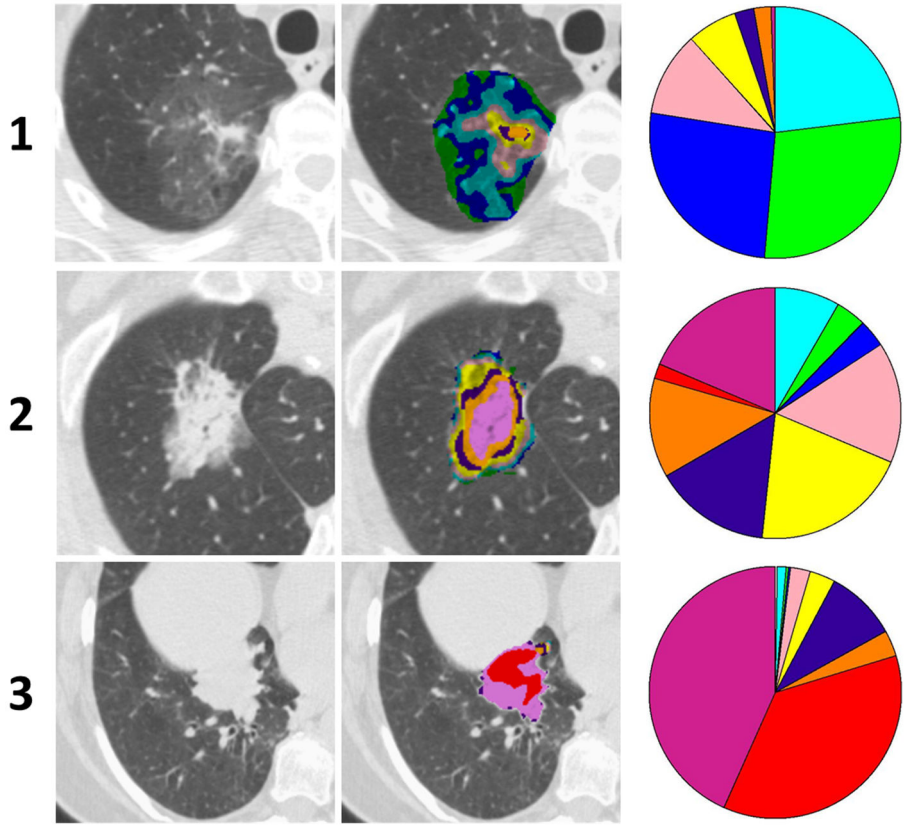

Figure 2.

The raw CT section, pattern overlay and glyph visualization of the three nodule exemplars identified by unsupervised affinity propagation (AP)-based clustering using pair-wise similarity of the parametric signatures.

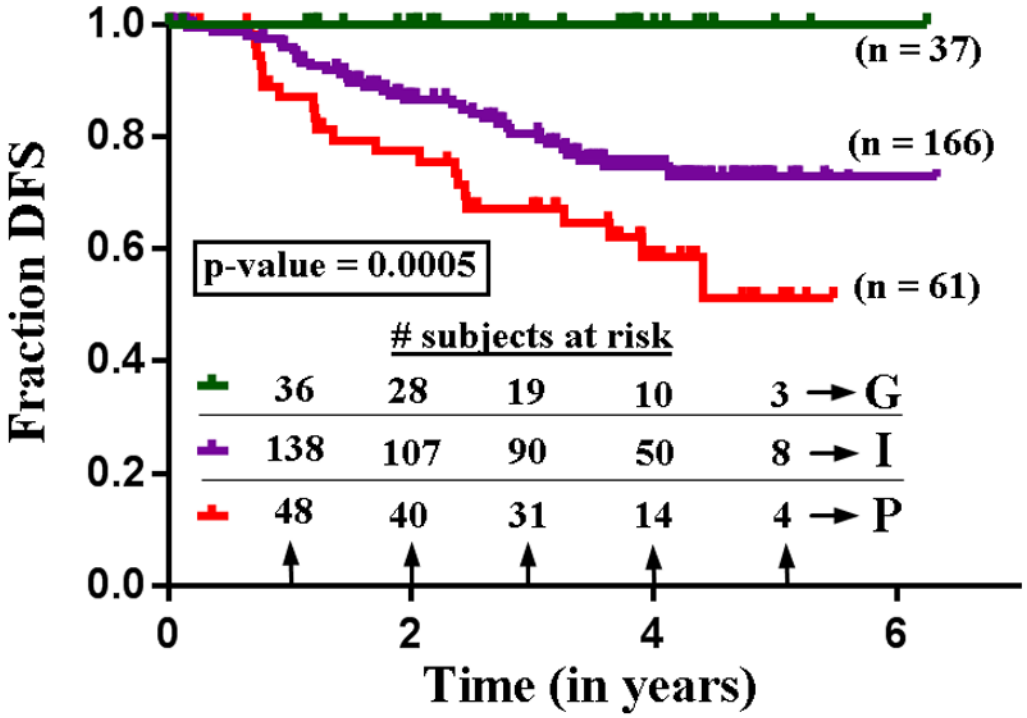

Figure 3.

Kaplan-Meier survival curve of 264 cases categorized into three automatically identified three groups of unique parametric signature.

Table 1

Patient demographics and pathological tumor stage.

Demographics	**N = 264**
Age at diagnosis Years: median (range)	68 (35–91)
Gender n (%) ***Women***	141 (53)
Smoking n (%) ***Never***	45 (17)
Pathologic TNM Stage n (%)	
I	216 (82)
II	22 (8)
III	23 (9)
IV	3 (1)

Table 2

Summary of effect of stratified clusters on outcomes adjusted by covariates using proportional fit model.

Effect likelihood ratio tests		
Variable	**Chi Square**	**p-value**
Age	1.22	0.26
Gender: Male vs Female	3.46	0.06
Smoking: Never vs current/former	3.36	0.06
Pathologic stage (I/II/III/IV)	2.08	0.55
Stratified groups (G/I/P)	19.75	<0.0001*